Journal of Materials Chemistry B

Accepted Manuscript

ROYAL SOCIETY OF CHEMISTRY

www.rsc.org/materialsB

Nanorod-aggregated flower-like CuO growing on carbon fiber fabric for a super high sensitive non-enzymatic glucose sensor

Weina Xu[1], Shuge Dai[1], Xue Wang[1,2,*], Xianming He[1], Mingjun Wang[1], Yi Xi[1], Chenguo Hu[1,*]

[1]*Department of Applied Physics, Chongqing University, Chongqing 400044, PR China*

[2]*School of Materials Science and Engineering, South China University of Technology, Guangzhou 510641, PR China*

[*]Corresponding author. Tel: +86 23 65678362; Fax: +86 23 65678362

E-mail address: hucg@cqu.edu.cn (CG Hu); msxw@scut.edu.cn (X Wang)

Abstract

A novel and exceptionally sensitive glucose biosensor based on nanorod-aggregated flower-like CuO growing on a carbon fiber fabric (CFF) is developed for glucose detection, which is prepared by a simple, fast and green hydrothermal method. The electron transfer resistance of the CuO/CFF electrode on the interface between electrode and electrolyte is as low as 12.79 Ω evaluated by electrochemical impedance spectroscopy. Cyclic voltammetry study reveals that the CuO/CFF electrode displays an excellent electrocatalytical activity toward the direct oxidation of glucose. Besides, chronoamperometry demonstrates a high sensitivity of 6476.0 μA mM^{-1} cm^{-2} at an applied potential of 0.45 V (vs. Ag/AgCl), with fast response time and low detection limit of only 1.3 s and ~ 0.27 μM. In addition, the glucose sensor has a high reproducibility with a relative standard deviation (R.S.D.) of 1.53% over eight identically fabricated electrodes and a long-term stability with a minimal sensitivity loss of ~ 9.9% over a period of one month as well as excellent anti-interference ability. Importantly, the CuO/CFF composite has such good flexible characteristics and can be manufactured into flexible electrodes for the application in various complicated circumstances. This work presents a new strategy to achieve highly sensitive glucose sensors with flexibility by growing glucose electroactive nanostructure materials directly on multichannel and high conductive carbon fiber fabric.

Keywords: Cupric oxide, carbon fiber fabric, non-enzymatic, glucose sensor, electrocatalysis

1 Introduction

As glucose oxidase-based sensors suffer from high-cost, complicated immobilization procedure, high overpotential for electrooxidizing glucose and insufficient stability originating from the intrinsic nature of enzyme molecules,[1] researchers pay more attention to non-enzymatic glucose sensors that do not compromise the excellent stability and high sensitivity, and get involved in the development of detecting the glucose level in human's blood and other practical applications.[2-5] However, up to now, electroactive materials of numerous non-enzymatic glucose biosensors have some disadvantages, such as poor electrical conductivity and electroactive sites. To overcome these disadvantages, high specific area supporting materials with excellent conductivity have attracted wide attention. Although carbon nanotubes and graphene with high conductivity and specific surface area are employed to support glucose electroactive materials, those materials do not have enough active sites to have sufficient contact with glucose due to their entanglement effect or ineffective channels. Therefore, it is important to explore a new substrate material with high electrical conductivity and multiple porous channels on which electroactive nanostructures could grow directly on it and form a large number of active sites. Carbon fiber fabric (CFF) is currently accepted as an excellent electrode material used in flexible solid state supercapacitors.[6-10] Carbon is highly conductive. CFF is interwoven by bundles of carbon fibers with multiple porous channels for liquid diffusion. Thus, they should be ideal supporting material for glucose sensors.

CuO,[11-12] MnO_2,[13] Co_3O_4,[14] NiO,[15] Ag_2O[16] etc., these transition metal oxides have been widely investigated for the development of non-enzymatic glucose sensors for their low cost, relatively high stability, excellent electrooxidation behavior of glucose at a lower overpotential. Among these various metal oxides, CuO, a p-type semiconductor with a narrow band gap of 1.2 eV, has been paid much attention to, due to its superior electrochemical and conductive activity, suitable surface charge and easily tunable surface structure. For example, CuO has been widely studied in supercapacitor,[17-18] lithium ion batteries,[19-20] gas sensors,[21-22] and photodetector[23]. Also CuO is extensively investigated for its applications in non-enzymatic glucose biosensing with fast responses and high sensitivity. For instance, Kun Li et al. reported that CuO nanoellipsoids modified electrode for non-enzymatic glucose detection exhibits a high sensitivity of 2555 $\mu A\ mM^{-1}\ cm^{-2}$, fast response time of ~3 s and good anti-interference ability.[24] In addition, carbonaceous materials, such as carbon nanotubes (CNTs), mesoporous carbons and graphene have emerged as intriguing electroactive materials due to their high electrical conductivity, high stability as well as relatively high mechanical properties.[25] In order to improve its sensitivity and conductivity of non-enzymatic glucose sensors, CuO/CNTs,[26] CuO/mesoporous carbons,[27] CuO/graphene[28] and CuO/graphene/CNTs[29] have been extensively investigated. However, the fabrication process of the CuO electrodes is not only time-consuming, but the cumbersome surface immobilization by surfactant, such as Nafion, prejudicing the charge transfer and involved ions diffusion from the support electrolyte to the electrode surface. Besides, the price of graphene and CNTs

is very high. Some efforts have been made in situ growth of CuO micro/nanostructures on Cu foils with lower-cost for sensitive enzyme-free determination of glucose.[11,30] For example, dandelion-like CuO micro/nanostructures growing on Cu foils were directly employed in detecting glucose concentration, which showed a remarkably high sensitivities 5368 μA mM^{-1} cm^{-2}.[11] But Cu foil is easily poisoned by chloride ions. Therefore, CuO nanostructure could be chosen as glucose electroactive material to grow directly on a multichannel and conductive substrate for highly sensitive non-enzymatic glucose sensing.

Herein, we demonstrate a simple and green synthesis of nanorod-aggregated flower-like CuO growing on CFF by the hydrothermal route at 100□ for 6 h. Although CuO nanocrystals, such as CuO nanoflowers,[2] CuO nanoellipsoids,[4] CuO nanoneedles,[29] CuO nanobelts,[30] CuO nanoparticles,[31] CuO nanowires,[32] CuO nanoplatelets[33] etc. have been synthesized, the synthesis of nanorod-aggregated flower-like CuO on CFF has not done yet. Non-enzymatic glucose sensor based on CuO growing directly on CFF (CuO/CFF) has not been reported previously. Compared with CNTs, CFF has such advantages as porous channels for liquid diffusion and high conductivity for charge transmission, low-cost and quantity production. As is expected, the as-prepared CuO/CFF electrode presents much higher sensitivity compared with other non-enzymatic glucose sensors reported previously.

2 Experimental section

2.1 Materials

Copper (II) acetate monohydrate ($(CH_3COO)_2Cu{\cdot}2H_2O$) was obtained from

Shanghai Qiangshun Chemical Company (Shanghai, China). Sodium hydroxide (NaOH), sodium chloride (NaCl), glucose, dopamine (DA), uric acid (UA), glutathione (GA), lactic acid (LA), were purchased from Chengdu Kelong Chemical Company (Chengdu, China). L-Ascorbic acid (AA), ethanol (CH_3CH_2OH) and nitric acid (HNO_3) were bought from Chongqing Chemical Reagent Company (Chongqing, China). Carbon fiber fabric was obtained from Shanghai Lishuo Composite Material Technology Company (Shanghai, China).

2.2 Synthesis of nanorod-aggregated flower-like CuO on CFF

The experimental steps are as follows: CFF with 2×4 cm^2 area was immersed in nitric acid solution for 4 h and then washed with deionized water for 5-6 times and finally dried in air at 60 °C for 30 min. $(CH_3COO)_2Cu \cdot 2H_2O$ (4 mmol) and NaOH (4 mmol) were respectively dissolved in the mixture of CH_3CH_2OH (10 mL) and deionized water (10 mL) under stirring; then NaOH solution was added dropwise to $(CH_3COO)_2Cu \cdot 2H_2O$ solution under stirring to form a milky blue thick solution. The CFF after above treatment was put into a Teflon vessel and the milky blue thick solution was also added to it, and then the vessel was put into stainless steel autoclave that subsequently was placed in a preheated furnace and maintained at 100 °C for 6 h. After a specific time, the Teflon vessel was taken out and let cool down to room temperature naturally. Finally, the prepared CFF covered with CuO (CuO/CFF) was taken out, and washed with deionized water and ethanol several times and dried in ambient air at 60 °C for 3 h. The nanorod-aggregated flower-like CuO growing on a single carbon fiber and on CFF are schematically illustrated in Fig. 1A and B,

respectively. From the comparison of the photographs between the bare CFF and the prepared CuO/CCF in Fig. 1B, we can see that the CuO/CCF has a dark black color with high flexibility. For comparison, pure CuO sample was also synthesized under the same condition except CFF was not added.

The mass loading of the CuO NFs was calculated by the difference in weight of the CuO/CFF (M) and bare CFF (m). To make the result reliable, twenty equivalent samples were weighed and then an average was taken. Finally, it was found that the mass loading of the CuO NFs is 0.36 mg/cm^2 for CuO/CFFs.

2.3 Electrode fabrication and electrochemical measurement

The working electrode for non-enzymatic electrochemical sensing was fabricated as follows: the CuO/CFF was directly connected with a copper wire by silver paste, where the connected part of the copper wire was pressed flat with a laminator. The edges and back of the electrode was covered by epoxy resin and an open active area of 1 cm × 1 cm was left. The CFF/CuO electrode was fabricated successfully without any surfactants. Similarly, the bare CFF electrode was prepared in the same way. For comparison, a graphite substrate (G) was polished to mirror smooth, rinsed with deionized water and ethanol, and then dried in air. Subsequently, a CuO/G electrode covered with about 0.36 mg mass loading of pure CuO NFs on its surface was fabricated and immobilized with polymer binder of 0.2 mL Nafion (0.25 wt%) solution. Electrochemical measurement was conducted by CHI 660D electrochemical workstation with a conventional three-electrode system in the supporting electrolyte of 100 mM NaOH aqueous solution. The CuO/CFF electrode was used as working

electrode, a platinum foil as counter electrode, a Ag/AgCl as reference electrode. Amperometric measurement was performed under a magnetically stirring condition for convective mass transport. A bare CFF electrode and CuO/G electrode were also measured for the purpose of comparison with the CuO/CFF electrode. All electrochemical measurements, including electrochemical impedance spectroscopy, cyclic voltammetry and chronoamperometry, were carried out at room temperature.

2.4 Characterization

X-ray diffraction (XRD, X'Pert PRO PHILIPS) was carried out to illustrate the structural and crystalline phase of the as-obtained samples using Cu K_α radiation in the range 10~80º. The surface morphology and size were observed by field emission scanning electron microscopy (FE-SEM, FEI NOVA 400) and energy dispersive X-ray spectroscopy (EDS, TESCAN VEGA 3 LMH SEM) was employed to analyze their chemical compositions.

3 Results and discussion

3.1 Morphology

Fig. 2A and B depict a low-magnification FE-SEM image of CuO nanostructure that has evenly grown on the surface of carbon fiber fabric substrate, which reveals that CFF substrate is an ideal matrix for the distribution of CuO. The scrape on the CCF demonstrates the coverage of CuO nanostructure. A high-magnification FE-SEM image of the as-prepared CuO is displayed in Fig. 2C. The detailed morphology of the synthesized CuO growing on CFF is shown in Fig. 2D, which displays that flower-like CuO consists of CuO nanorod aggregation with an average rod diameter

of ~ 10 nm. And the pure CuO sample also has a flower-like structure assembled by CuO nanorods (Fig. S1a-b).

3.2 XRD pattern analysis

The XRD pattern in Fig. 3A demonstrates that the nanostructure growing on carbon fiber fabric has CuO phase (JCPDS No. 74-1021, a = 4.653 Å, b = 3.410 Å, c = 5.108 Å, C2/c(15)). The additional diffraction angle at 2θ = 26.309º coming from carbon fiber fabric matches well with (111) plane of rhombohedral carbon (JCPDS No. 75-0444, a = 3.635 Å, 3.635 Å, 3.635 Å, R-3m(166)). No other diffraction peaks of impurities such as Cu_2O, $Cu(OH)_2$ are detected, which shows the as-prepared sample is only CuO. The EDS analysis reveals that the as-prepared sample is mainly oxygen and copper and the peak of carbon comes from carbon fiber fabric, as depicted in Fig. 3B.

4 Glucose sensor

4.1 Electrochemical properties of CuO/CFF and CFF electrodes

Electrochemical impedance spectroscopy (EIS) measurement is usually used to study the electron transfer between the electrolyte and the electrode surface. Typical Nyquist plot is composed of a semicircle section in high frequency controlled by electron transfer process and a linear region with a 45º slope in low frequency controlled by diffusion process in the electrochemical process. The semicircle diameter represents the electron transfer resistance (R_{et}) on the interface between electrode and electrolyte. The Nyquist plots of CuO/CFF, CuO/G and CFF electrodes are tested in 100 mM NaOH solution at the frequency range from 1 Hz to 10^5 Hz,

shown in Fig. 4. As is expected, the complex impedance plot of bare CFF electrode reveals that its semicircle diameter in high frequency region is smaller compared with that of the CuO/CFF electrode, which indicates that the modification of CuO on CFF hinders the electron transfer process and increases the electron transfer resistance. The change of the electron transfer resistance illustrates that CuO nanomaterial grows on CFF successfully. The inset drawn by ZsimpWin instrument represents the proposed equivalent circuit obtained by fitting to the experimental data. In the circuit, R_s stands for the Ohmic resistance of the solution and underlying electrode, R_{et} for the electron transfer resistance, C_d for capacitance on the interface, CPE_1 for constant phase angle element instead of double-layer capacitance on the modified electrode between electrode and electrolyte and R_1 for the adsorption resistance caused by the adsorption of NaOH to CuO/CFF, CuO/G or CFF, respectively. By simulation calculation, the electron transfer resistance (R_{et}) increases from 7.95 Ω for the CFF to 12.79 Ω for the CuO/CFF composite, and the R_{et} for the CuO/G electrode is 15.31 Ω. Obviously, the R_{et} for the CuO/CFF electrode is smaller than that of the CuO/G electrode, which shows that CuO directly growing on CFF improves electron transfer rate for the interconnected porous channels of the conductive carbon fiber facilitate the mass transfer of the electrolyte. And the ohmic resistance (R_s) is 0.45 Ω, 0.67 Ω and 4.69 Ω for CFF, CuO/CFF and CuO/G electrodes, respectively. The R_s for CuO/CFF electrode is also smaller than that of CuO/G electrode, which results from the decrease of the contact resistance at the interface of the electroactive material and electrolyte due to the binder-free structure, and the contact resistance between CuO

and CCF.

4.2 Electrocatalysis of glucose on CFF and CuO/CFF electrodes

Cyclic voltammetry (CV) is measured to test the electrocatalytic activity of the pure CFF, CuO/CFF and CuO/G electrodes towards glucose oxidation in an alkaline medium. Fig. 5 shows the successive CVs of the pure CFF, CuO/CFF and CuO/G electrodes without and with successive addition of 1 mM glucose (from 1 mM to 3 mM) to 100 mM NaOH solution at the scan rate of 50 mV s^{-1}. As is shown in Fig. 5A, no redox peaks can be observed in the absence and presence of glucose for the pure CFF electrode, which reveals that the CFF electrode has no electrocatalytical activity toward the direct oxidation of glucose. However, the CuO/CFF and CuO/G electrodes display a relatively broad reduction peak with the potential of ~ 0.30 V (vs. Ag/AgCl) without the presence of glucose, which is ascribed to the Cu(II)/Cu(III) redox couple,[28,29] and there is no distinct oxidation peak observed in the potential window which could be overlaid by the oxidation peak of water-splitting,[3] as are shown in Fig. 5B-C. For the CuO/CFF electrode, the current density increases proportionally with the successive addition of 1.0 mM glucose to 100 mM NaOH solution at ~ 0.45 V (vs. Ag/AgCl), but a gradual increase in the current density for the CuO/G electrode is not proportional to the increase of glucose concentration, which suggests that the CuO/CFF electrode could not be poisoned by oxidation products and keeps a good stability. The detail comparison of the electrocatalytic properties of the CuO/CFF electrode with CuO/G electrode is shown by CV in 100 mM NaOH solution with 1.0 mM glucose (Fig. S2), indicating the higher oxidation peak current for the CuO/CFF

electrode. It is clear that the CuO/CFF electrode has an excellent electrocatalytical activity toward the direct oxidation of glucose, for the CuO/CFF nanostructure has advantages of the high specific surface area and porous channels, which provide large electroactive sites and improve electron transfer rate due to direct electron collection by the conductive carbon fiber. The possible mechanism of the direct electro-oxidation of glucose in the alkaline medium is presented in Scheme 1.[2-4,34-35] The increase of oxidation current is mainly ascribed to the fact CuO is oxidated to CuOOH or $Cu(OH)_4^-$ on the surface of CuO/CFF electrode (equation (I)), and then glucose is catalytically oxidized to glucolactone and further to gluconic acid by hydrolyzation process (equation (II)).[34]

In order to know the electrochemical kinetics for catalytic oxidation of glucose, the CV curves of the CuO/CFF electrode in 100 mM NaOH solution containing 1.0 mM glucose at various scan rates ranging from 10 to 100 mV s^{-1} are measured, as is depicted in Fig. 6. For the CuO/CFF electrode, the cathodic peak potential shifts negatively with the increase in scan rate, as is shown in Fig. 6A. Furthermore, the cathodic peak current (I_{pc}) steadily decreases with the increase of scan rate. Fig. 6B shows that the cathodic peak currents are linearly proportional to the square root of scan rate, which can be expressed with linear regression equation: I_{pc} (mA) = -1.3022 $v^{1/2}$ + 2.6632 with a correlation coefficient (R^2>0.989). It indicates that the redox reaction of the electrode is a diffusion-controlled electrochemical process.[36]

4.3 Optimization of glucose sensor performance

Various factors affecting sensitivity of the sensor, such as the concentration of

NaOH and the applied potential, are taken into account for the purpose of improving its performance. It is well-known that OH^- ions play a vital role in the electrocatalytic oxidation of glucose on the CuO/CFF electrode. So, the concentration of NaOH for the glucose sensor should be optimized. Fig. 7A displays the CVs of CuO/CFF electrode in different NaOH concentrations (10 mM, 50 mM, 100 mM, 150 mM, 200 mM) with 1.0 mM glucose at 50 mV s^{-1}. The oxidation peak current at first increases dramatically and afterwards decreases slowly with the increase of NaOH concentration. And Fig. 7B depicts that the anodic peak potential shifts to more negative potential with the increase of NaOH concentration from 10 to 100 mM and then the potential shifts to more positive, and that the oxidation current response in 100 mM NaOH solution reaches the maximum in a lower peak potential at ~ 0.45 V. Thus, 100 mM NaOH is selected as the optimal support electrolyte for further work.

Besides, the optimal potential for improving the sensitivity of glucose sensing is investigated by chronoamperometry. Fig. 7C illustrates the amperometric response at CuO/CFF electrode with successive injection of 40 μM glucose into 100 mM NaOH every 50 s under applied different potentials from 0.35 V to 0.60 V (vs. Ag/AgCl). As is shown in Fig. 7D, the response current increases firstly along with increase in the applied potential up to 0.45 V and then decreases sharply with the further increase in the applied potential from 0.45 V to 0.6 V. That is to say, the response current reaches the maximum value at 0.45 V, with a good signal-to-background ratio, which is consistent with the result of CV (Fig. 5B). The above results may come from the reason that relatively high potential would activate some interfering species that are

stable under low potential and generate many intermediates that would probably interact with the electrode material to hinder the glucose oxidation and even harm the electrode.[11,31,33] Thus, 0.45 V is chosen as the optimal potential for the amperometric glucose sensor.

4.4 Amperometric detection of glucose sensor

The amperometric responses are employed to monitor the detection of glucose on the CFF, CuO/G and CuO/CFF electrodes for successive addition step-wise change of glucose concentrations in 100 mM NaOH solution at 50 s intervals under an applied potential of 0.45 V (vs. Ag/AgCl), as is shown in Fig. 8A. The bare CFF electrode (curve a) presents few amperometric responses to the successive addition of glucose. By contrast, the CuO/G electrode (curve b) and CuO/CFF electrode (curve c) shows remarkably high current responses to the successive addition of glucose. Moreover, the intensity of response current toward the oxidation of glucose increases with the increase in concentration of glucose from 0.3 μM to 1.04 mM. Obviously, with an increase in concentration of glucose and reaction time, the noise increases because the electrode adsorbs more and more intermediate species. Fig. 8C displays the response curves of the CuO/G (curve b) and CuO/CFF (curve c) toward low concentrations of glucose ranging from 0.3 μM to 40 μM. It can be noted that an obvious response is observed at the CuO/G and CuO/CFF by addition of 0.3 μM glucose. Furthermore, Glucose sensors on the CuO/G (curve b) and CuO/CFF (curve a) have a linear relationship between the oxidation current and glucose concentration ranging from 0.3 μM ~ 0.96 mM, observed in Fig. 8B, which is expressed by linear

regression equation: I_{pa} (mA) = 4.5427Gc (mM) -0.0286 (curve b), with a sensitivity of 4542.7 μA mM^{-1} cm^{-2} and a correlation coefficient of 0.9953 and I_{pa} (mA) = 6.4760Gc (mM) + 0.0069 (curve c), with a sensitivity of 6476.0 μA mM^{-1} cm^{-2} and a correlation coefficient of 0.9977. Fig. 8D shows the linear relationship between the oxidation current and low concentrations of glucose ranging from 0.3 μM ~ 40 μM. Importantly, the current on the CuO/CFF quickly reaches a steady value within only 1.3 s (inset in Fig. 8A) to the successive addition of glucose, while the current on the CuO/G reaches a steady value within 2.1 s (inset in Fig. 8C), demonstrating a faster amperometric response behavior to glucose on the CuO/CFF than that on the CuO/G. All these observations indicate that CuO/CFF exhibits an more excellent electrocatalytic ability toward oxidation of glucose than CuO/G. The sensitivity of the non-enzymatic glucose sensor based on the CuO/CFF is much higher than that of those similar sensors reported before.[37-40] Furthermore, the lower detection limit of the biosensor is ~ 0.27 μM based on a signal/noise ratio of 3. The influence of the mass loading of CuO on CFF towards the electrocatalytic oxidation of glucose is investigated, and the amperometric responses of the CuO/CFF electrodes to successive additions of glucose at the potential of 0.45 V are shown in Fig. S3a-b. The morphologies of the different CuO mass loadings are characterized by SEM images in Fig. S4a-c. Table 1 summarizes the analytical parameters of the CuO/CFF electrodes for different mass loadings, indicating 0.36 mg/cm^2 mass loading is the best.

Table 1. The influence of the mass loading of CuO growing on CFF towards the direct oxidation of glucose.

Samples	Mass loading (mg/cm^2)	Linear range (mM)	Sensitivity ($\mu A\ mM^{-1}\ cm^{-2}$)
4h	0.28	0.84	5259.4
6h	0.36	0.96	6476.0
8h	0.45	0.96	5827.7

The performances of the CuO/CFF electrode, including response time, detection limit, sensitivity, linear range and applied potential, are compared with other cupric oxide-based and other materials-based non-enzyme glucose sensors reported in literatures in Table 2. From the comparative data, it can be deduced that the CuO/CFF electrode exhibits such superior performance as ultra high sensitivity, low detection limit and low applied potential towards the glucose oxidation, which can be attributed to the fact that the nanorods-aggregated flower-like CuO directly growing on CFF. CuO/CFF has high specific surface area and porous channels which provide the large electroactive sites and improve electron transfer rate due to the directly electron collection by the conductive carbon fiber.

Table 2. Comparison of the performances of sensing based on CuO/CFF electrode with other non-enzyme glucose sensors based CuO and other materials reported in literatures.

Electrode material	Response time (s)	Detection limit (μM)	Sensitivity ($\mu A\ mM^{-1}\ cm^{-2}$)	Linear range (up to, mM)	Potential (V)	Reference
CuO/CFF	1.3	0.27	6476.0	0.96	0.45	This work
Sandwich-structured CuO	0.7	1.0	5342.8	0.7	0.6	[2]
CuO nanoellipsoids	3	0.072	2555	3	0.55	[24]
CuO nanoplatelets	~	0.5	3490.7	0.8	0.55	[33]
Flower-like CuO	5	0.5	5368	1.6	0.6	[11]
CuO NFs-ITO	<1	0.04	873	1.3	0.48	[37]

CuO nanoparticles	~	0.2	2596	1.2	0.4	[38]
CuO nanosheets/Cu	2.2	0.8	2792.6	2.2	0.5	[39]
Porous Co_3O_4	3	~	471.5	12.5	0.59	[40]
Fe_2O_3 nanowires	<6	15	726.9	8	0.55	[41]
$Ni(OH)_2$nanoparticles	~	0.53	2400	15	0.53	[42]
MoS2 nanosheet	2	0.31	1824	4	0.5	[43]
Hollow cage-like NiO	3.3	0.1	2476.4	5	0.48	[44]
RGO/$Ni(OH)_2$	7	15	11400	30	0.6	[45]
Pd/MWCNTs	1	0.2	1275	22	-0.4	[46]

4.5 Reproducibility, stability and anti-interference and anti-poisoning properties

Higher reproducibility and long-term stability of sensors are of critical importance for practical detection application. In this paper, the stability of glucose sensor on the CuO/CFF is tested by measuring its amperometric current response to glucose during a period of 30 days at a time interval of a day. Fig. 9A reveals that the sensitivity of the prepared electrode still keeps approximately 90.1% of its original current response after one month, which can be ascribed to the strong adhesion of CuO on carbon fiber fabric and the chemical stability of CuO in basic solution. As for the reproducibility, eight CuO/CFF electrodes fabricated independently under the same conditions, are employed to test their amperometric current responses for the addition of 0.1 mM glucose into 100 mM NaOH at applied potential of 0.45 V (vs. Ag/AgCl). As is shown in the inset of Fig. 9A, they have an average oxidation current of 0.94 mA with a relative standard deviation (R.S.D.) of 1.53%, indicating that the fabrication method of the CuO/CCF electrode has a high reproducibility.

Anti-interference and poison resistance of chloride ions are two of important factors that are used to determine reproducibility, stability and inaccuracy of

non-enzymatic glucose sensors. It is common knowledge that some interfering agents usually coexist with glucose in human blood; they are ascorbic acid (AA), dopamine (DA), uric acid (UA), glutathione (GA) and lactic acid (LA), and chloride ions such as NaCl. Previous literatures reported that the concentration of interfering species in human blood is about 30 times less than that of glucose,[39] thus the ratio of concentration between glucose and interfering species (glucose : species = 10:1) in the present situation is used to detect the resistant to interference. As is shown in Fig. 9B, the amperometric response current of the CuO/CFF electrode towards glucose sensor is examined by the dropwise addition of 100 μM glucose (Gc), 10 μM interfering species respectively. The inset in Fig. 9B shows that the ratio of response current of interfering agents to that of glucose is 1.02% for AA, 1.01% for DA, 2.03% for UA, 1.92% for LA, 3.67% for GA and 1.01% for NaCl, respectively, and the sensitivity of the CuO/CFF electrode towards glucose has only 2.38% loss after the presence of interfering species, indicating that the CuO/CFF sensing reveals good selectivity for glucose detection.

4.6 Real blood analysis

The CuO/CFF is also applied to detect the concentration of glucose in human blood and the corresponding results are shown in table S1. The CuO/CFF electrode presents a good recovery of glucose by addition of 0.1 mM glucose to the solutions containing the serum, indicating that the electrode can be used as an amperometric sensor for determination of glucose level in real blood serum samples.

5 Conclusions

In summary, nanorod-aggregated flower-like CuO has firmly grown on carbon fiber fabric by a simple, fast and green hydrothermal method. The as-prepared CuO/CFF composite can be directly fabricated into glucose biosensors for detecting glucose, which exhibits such striking characteristics as high sensitivity of 6476.0 μA mM^{-1} cm^{-2}, low applied potential of 0.45 V, fast response time of only 1.3 s, low detection limit of ~ 0.27 μM, and long-term stability with a minimal sensitivity loss of ~ 9.9% over a period of one month, besides admired anti-interference ability and splendid reproducibility with a relative standard deviation of 1.53%. This is mainly ascribed to the high specific surface area provided by the nanorod-aggregated flower-like CuO structure and the acceleration of electron transfer rate from the porous channels and directly electron collection by the conductive carbon fiber. The results indicate that CuO/CFF hybrid nanocomposite is an attractive material for the construction of superior amperometric glucose sensors. The great flexibility of CuO/CFF nanostructure is another striking advantage and can be applied to various complicated circumstances on exploring the various structure designs of glucose biosensors.

Acknowledgements

This work is supported by the National High Technology Research and Development Program of China (SQ2015AA034801), NSFC (11204388, 51402112), SRFDP (20120191120039), and the Fundamental Research Funds for the Central Universities (CQDXWL-2014-001 and CQDXWL-2013-012).

References

1 S. B. Bankar, M. V. Bule, R. S. Singhal and L. Ananthanarayan, *Biotechnol. Adv.*, 2009, **27**, 489-501.

2 S. K. Meher and G. R. Rao, *Nanoscale*, 2013, **5**, 2089-2099.

3 S. Liu, Z. Y. Wang, F. J. Wang, B. Yu and T. Zhang, *RSC Adv.*, 2014, **4**, 33327-33331.

4 X. Z. Zhang, S. D. Sun, J. Lv, L. L. Tang, C. C. Kong, X. P. Song and Z. M. Yang, *J. Mater. Chem. A*, 2014, **2**, 10073-10080.

5 X. Wang, C. G. Hui, H. Liu, G. J. Du, X. S. He and Y. Xi, *Sens. Actuator B-Chem.*, 2010, **144**, 220-225.

6 X. Cai, M. Peng, X. Yu, Y. P. Fu and D. C. Zou, *J. Mater. Chem. C*, 2014, **2**, 1184-1200.

7 Q. Yang, X. T. Zhang, M. Y. Zhang, Y. Gao, H. Gao, X. C. Liu, H. Liu, K. W. Wong and W. M. Lau, *J. Power Sources*, 2014, **272**, 654-660.

8 X. H. Lu, T. Zhai, X. H. Zhang, Y. Q. Shen, L. Y. Yuan, B. Hu, L. Gong, J. Chen, Y. H. Gao, J. Zhou, Y. X. Tong and Z. L. Wang, *Adv. Mater.*, 2012, **24**, 938-944.

9 H. Qian, A. R. Kucernak, E. S. Greenhalgh, A. Bismarck and M. S. P. Shaffer, *ACS Appl. Mater. Interfaces*, 2013, **5**, 6113-6122.

10 L. Y. Yuan, X. H. Lu, X. Xiao, T. Zhai, J. J. Dai, F. C. Zhang, B. Hu, X. Wang, L. Gong, J. Chen, C. G. Hu, Y. X. Tong, J. Zhou and Z. L. Wang, *ACS Nano*, 2012, **6**, 656-661.

11 K. Li, G. L. Fan, L. Yang and F. Li, *Sens. Actuator B-Chem.*, 2014, **199**, 175-182.

12 R. Khan, M. Vaseem, L. W. Jang, J. H. Yun, Y. B. Hahn and I. H. Lee, *J. Alloy. Compd.*, 2014, **609**, 211-214.

13 Z. C. Meng, Q. L. Sheng and J. B. Zheng, *J. Iran Chem. Soc.*, 2012, **9**, 1007-1014.

14 C. Y. Guo, X. Zhang, H. H. Huo, C. L. Xu and X. Han, *Analyst*, 2013, **138**, 6727-6731.

15 C. Dhand, M. Das, M. Datta and B. D. Malhotra, *Biosens. Bioelectron.*, 2011, **26**, 2811-2821.

16 Z. Y. Jin, P. P. Li, B. Z. Zheng, H. Y. Yuan and D. Xiao, *Anal. Methods*, 2014, **6**, 2215-2220.

17. K. Krishnamoorthy, S.-J. Kim, *Mater. Res. Bul.*, 2013, **48**, 3136 – 3139.

18. D. T. Pham, T. H. Lee, D. H. Long, F. Yao, A. Ghosh, V. T. Le, T. H. Kim, B. Li, J. Chang, and Y. H. Lee, *ACS Nano*., 2015, **9**, 2018-2027.

19. N. Ozer and F. Tepehan, *Sol. Energ. Mat. Sol. C.*, 1993, **30**, 13-26.

20. A. S. Zoolfakar, R. A. Rani, A. J. Morfa, A. P. O'Mullane and K. K. Zadeh, *J. Mater. Chem. C*, 2014, **2**, 5247-5270.

21. A. S. Zoolfakar, M. Z. Ahmad, R. A. Rani, J. Z. Ou, S. Balendhran, S. Zhuiykov, K. Latham, W. Wlodarski and K. Kalantar-zadeh, *Sens. Actuators B*, 2013, **185**, 620-627.

22. H. Kim, C. Jin, S. Park, S. Kim and C. Lee, *Sens. Actuators B*, 2012, **161**,

594-599.

23. B. J. Hansen, N. Kouklin, G. Lu, I. K. Lin, J. Chen and X. Zhang, *J. Phys. Chem. C*, 2010, **114**, 2440-2447.

24 H. G. Nie, Z. Yao, X. M. Zhou, Z. Yang and S. M. Huang, *Biosens. Bioelectron.*, 2011, **30**, 28-34.

25 N. Saito, K. Aoki, Y. Usui, M. Shimizu, K. Hara, N. Narita, N. Ogihara, K. Nakamura, N. Ishigaki, H. Kato, H. Haniu, S. Taruta, Y. A. Kim and M. Endo, *Chem. Soc. Rev.*, 2011, **40**, 3824-3834.

26 H. X. Wu, W. M. Cao, Y. Li, G. Liu, Y. Wen, H. F. Yang and S. P. Yang, *Electrochim. Acta*, 2010, **55**, 3734-3740.

27 J. Zhang, N. N. Ding, J. Y. Cao, W. C. Wang and Z. D. Chen, *Sens. Actuator B-Chem.*, 2013, **178**, 125-131.

28 Y. W. Hsu, T. K. Hsu, C. L. Sun, Y. T. Nien, N. W. Pu and M. D. Ger, *Electrochim. Acta*, 2012, **82**, 152-157.

29 D. X. Ye, G. H. Liang, H. X. Li, J. Luo, S. Zhang, H. Chen and J. L. Kong, *Talanta*, 2013, **116**, 223-230.

30 T. Soejima, H. Yagyu, N. Kimizuka and S. Ito, *RSC Adv.*, 2011, **1**, 187-190.

31 J. Yang, L. C. Jiang, W. D. Zhang and S. Gunasekaran, *Talanta*, 2010, **82**, 25-33.

32 D. Q. Huo, Q. Li, Y. C. Zhang, C. J. Hou and Y. Lei, *Sens. Actuator B-Chem.*, 2014, **199**, 410-417.

33 J. Wang and W. D. Zhang, *Electrochim. Acta,* 2011, **56**, 7510-7516.

34 S. D. Sun, X. Z. Zhang, Y. X. Sun, S. C. Yang, X. P. Song and Z. M. Yang, *ACS Appl. Mater. Interfaces*, 2013, **5**, 4429-4437.

35 J. F. Huang, Y. H. Zhu, X. L. Yang, W. C., Y. Zhou and C. Z. Li, *Nanoscale*, 2015, **7**, 559-569.

36 Y. Mu, D. L. Jia, Y. Y. He, Y. Q. Miao and H. L. Wu, *Biosens. Bioelectron.*, 2011, **26**, 2948-2952.

37 G. Y. Liu, B. Z. Zheng, Y. S. Jiang, Y. Q. Cai, J. Du, H. Y. Yuan and D. Xiao, *Talanta*, 2012, **101**, 24-31.

38 L. C. Jiang and W. D. Zhang, *Biosens. Bioelectron.*, 2010, **25**, 1402-1407.

39 L. L. Tian and B. T. Liu, *Appl. Surf. Sci.*, 2013, **283**, 947-953.

40 L. Han, D. P Yang, A. H. Liu, Biosens. Bioelectron., 2015, **63**, 145-152.

41 X. Cao and N. Wang, *Analyst*, 2011, **136**, 4241-4246.

42 M. A. Kiani, M. Abbasnia Tehrani, H. Sayahi , *Anal. Chim. Acta*, 2014, **839**, 26-33.

43 J. W. Huang, Y.Q. He, J. Jin, Y.R. Li, Z.P. Dong, R. Li, *Electrochim. Acta*, 2014, **136**, 41-46.

44 Z. H. Ibupoto, A. Nafady, R. A. Soomro, S. T. H. Sherazi, M. I. Abro and M. Willander, *RSC Adv.*, 2015, **5**, 18773-18781.

45 P. Subramanian, J. N. Jonsson, A. Lesniewski, Q. Wang, M. S. Li, R. Boukherroub and S. Szunerits, *J. Mater. Chem. A*, 2014, **2**, 5525-5533.

46 B. Singh, N. Bhardwaj, V.K. Jain, V. Bhatia, Sensor. Actuat. A, 2014, **220**, 126-133. 46 Y. Ding, Y. Wang, L. A. Su, M. Bellagamba, H. Zhang and Y.

Lei, *Biosens. Bioelectron.*, 2010, **26**, 542-548.

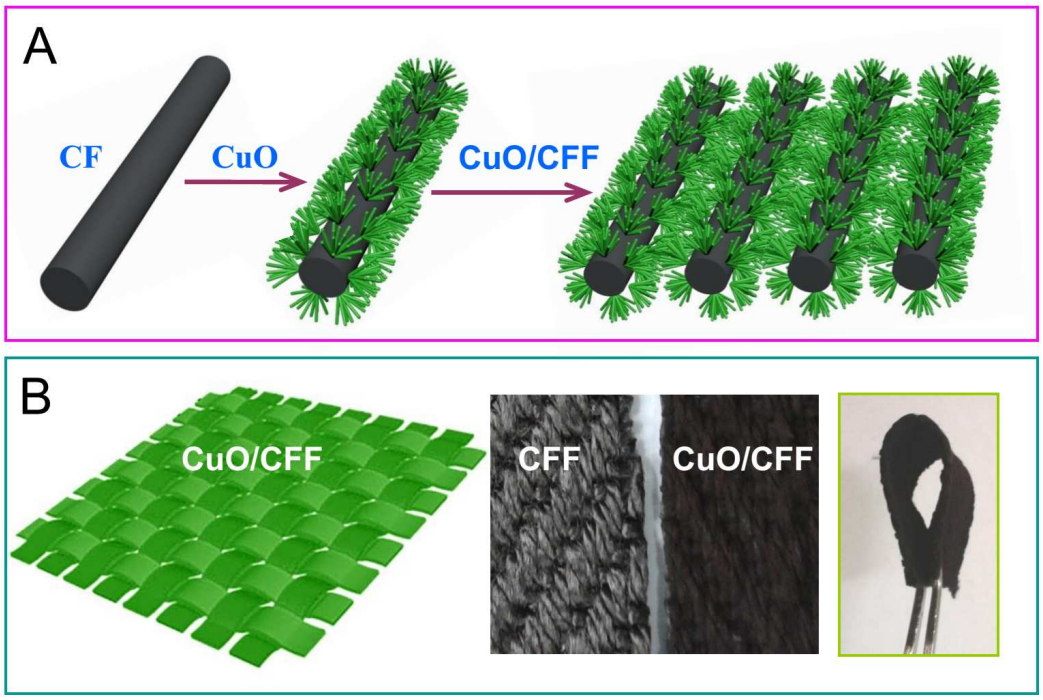

Fig. 1 (A) Schematic illustration of the preparation process of nanorod-aggregated flower-like CuO composite and (B) the planimetric map of CuO/CCF composite, the photos of the CCF and CuO/CCF composite, displaying the different color and flexibility.

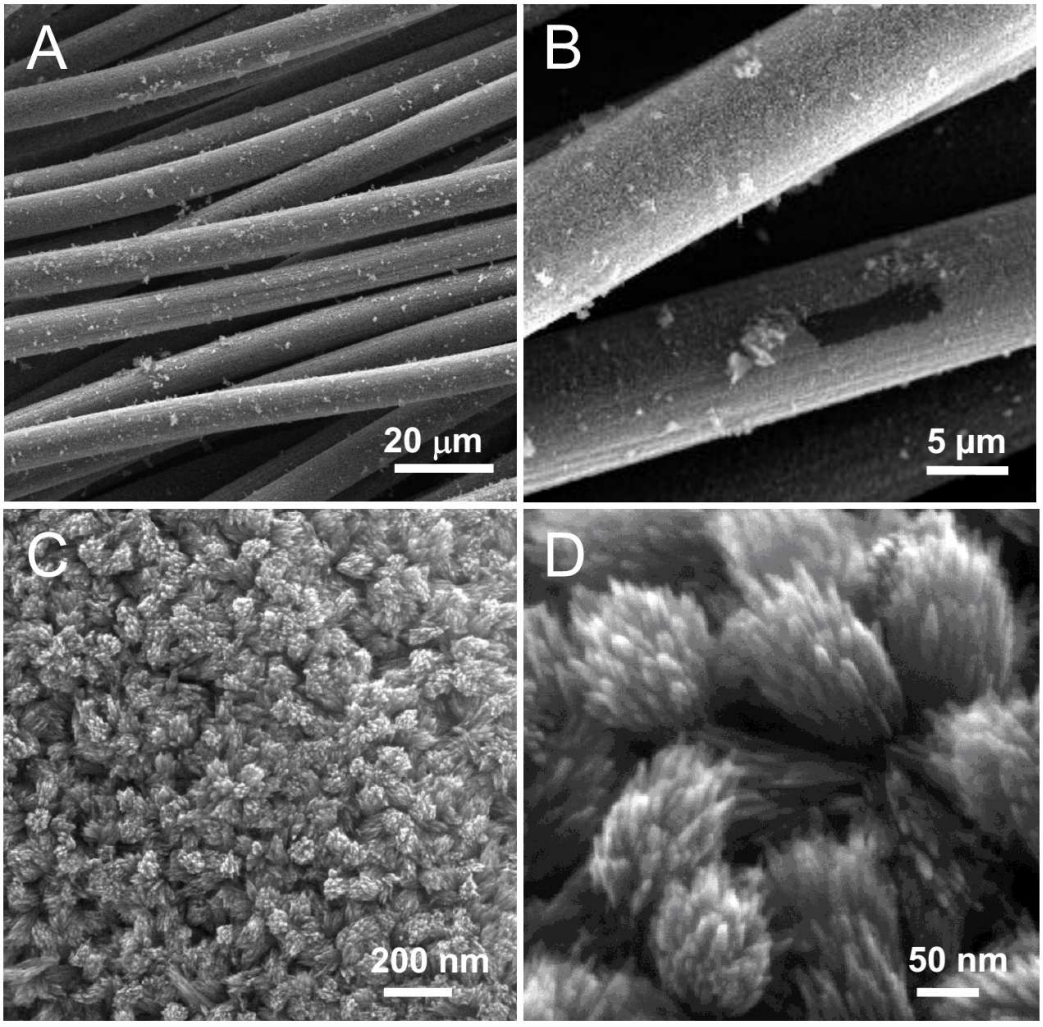

Fig. 2 Low-magnification FE-SEM images (A) and (B); high-magnification FE-SEM image (C); detailed morphology image (D) of CuO grown on CFF composite.

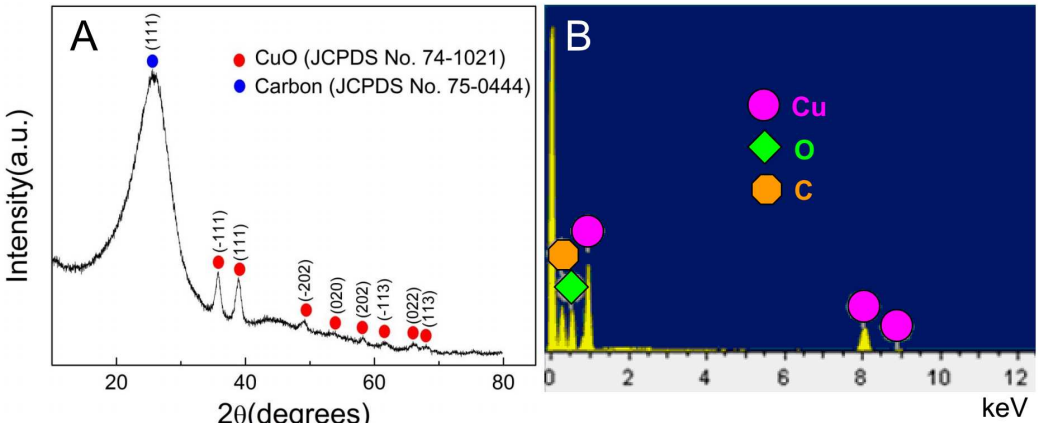

Fig. 3 XRD pattern (A) and EDS spectrum (B) of the CuO/CCF composite.

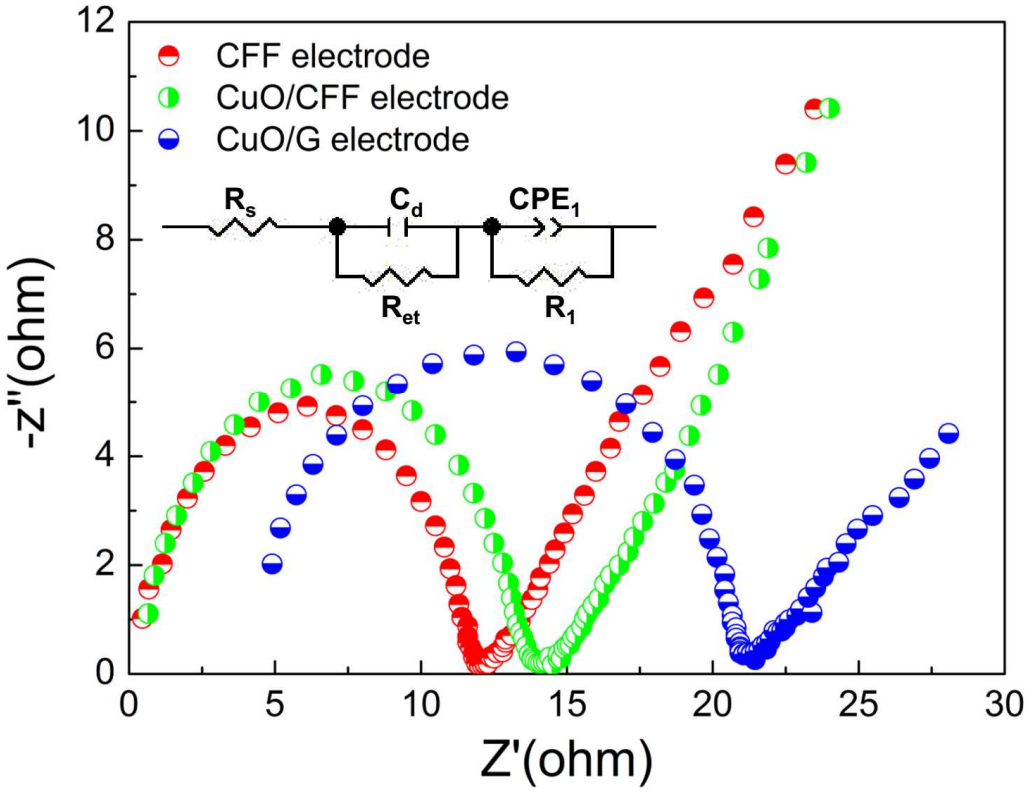

Fig. 4 EIS results of bare CFF, CuO/G and CuO/CFF electrodes in 100 mM NaOH solution. Inset in the upper center is the proposed equivalent circuit.

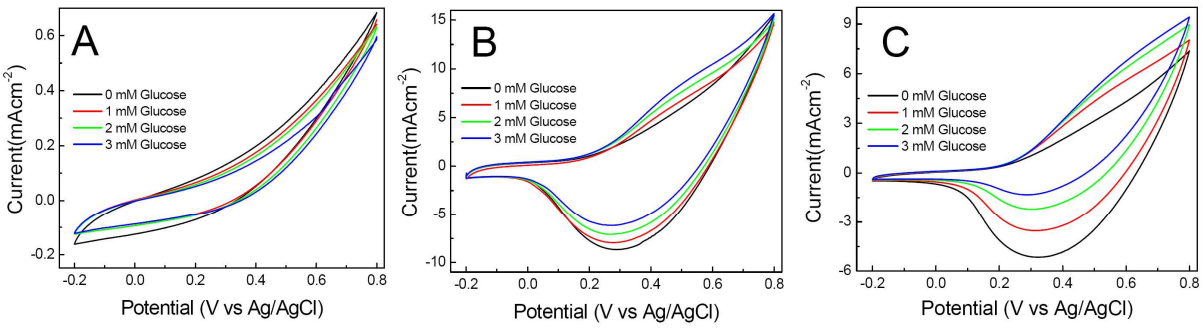

Fig. 5 The successive CVs of the CFF electrode (A), CuO /CFF electrode (B) and CuO/G electrode (C) without and with successive addition of 1.0 mM glucose in 100 mM NaOH solution at 50 mV s^{-1}.

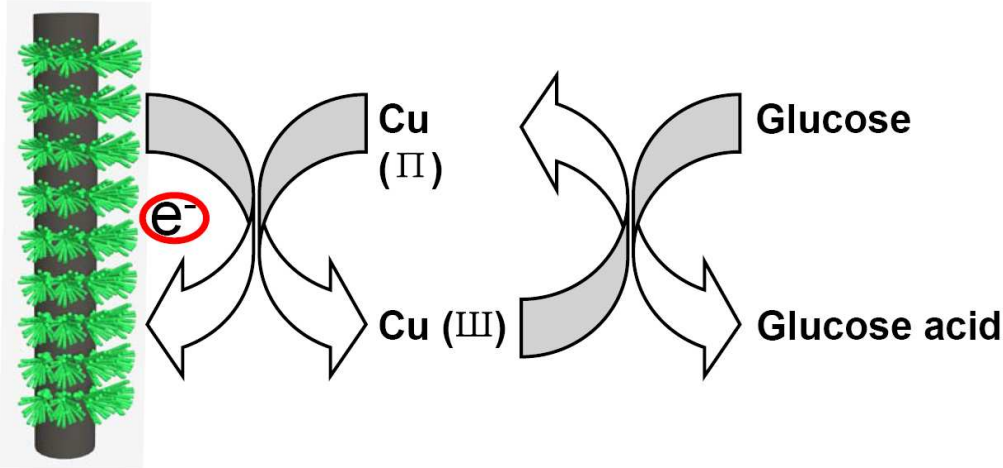

Ⅰ) $CuO + OH^- \longrightarrow CuOOH + e^-$

$CuO + H_2O + OH^- \longrightarrow Cu(OH)_4^- + e^-$

Ⅱ) $Cu(Ⅲ) + e^- + glucose \longrightarrow Clucolactone + CuO$

$Clucolactone \xrightarrow{hydrolyzation} Gluconic\ acid$

Scheme1 The possible mechanism of the direct electro-oxidation of glucose to gluconic acid on CuO/CFF electrode surface in the alkaline medium.

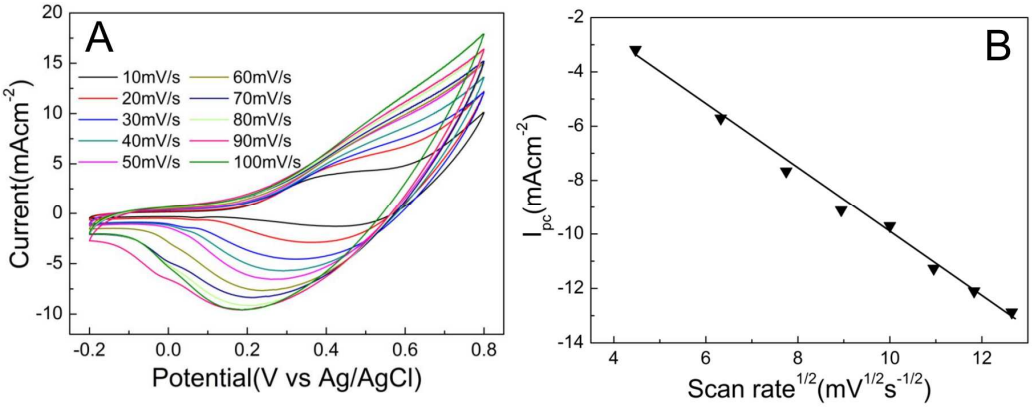

Fig. 6 CVs of CuO/CFF electrode at different scan rates from 10 to 100 mV s^{-1} in 100 mM NaOH solution containing 1.0 mM glucose (A); plots of cathodic peak current versus the square root of scan rate (B).

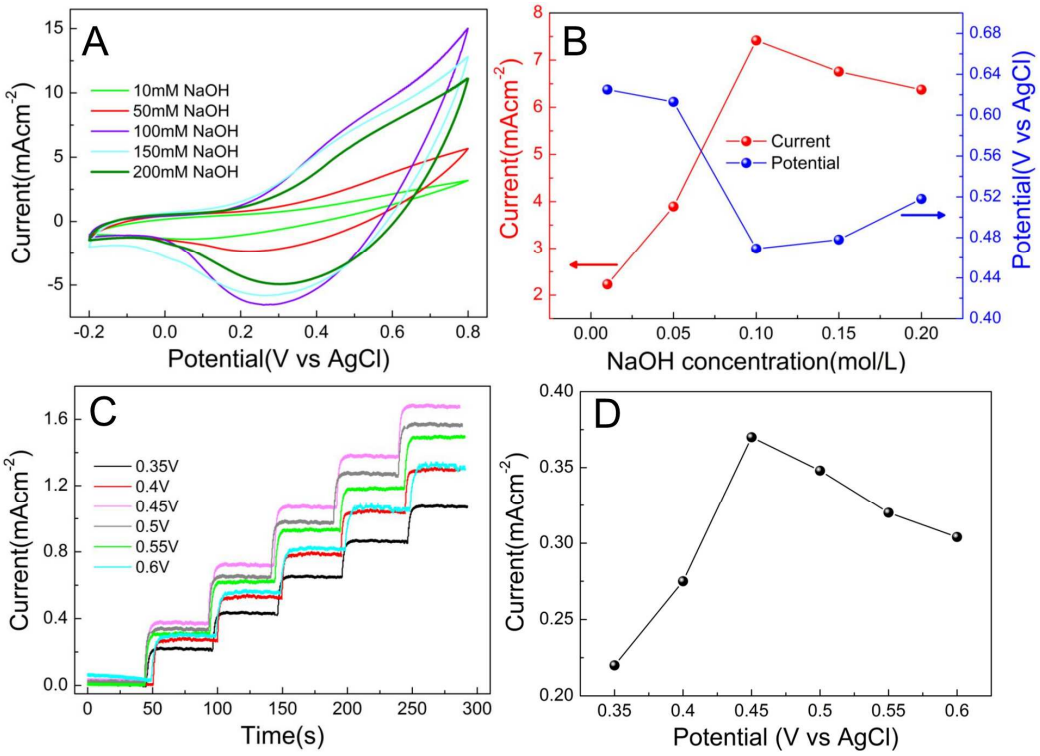

Fig. 7 (A) CVs of CuO/CFF electrode in different NaOH concentration with 1.0 mM glucose at 50 mV s^{-1}; (B) effect of NaOH concentration on peak current and peak potential of CuO/CFF electrode; (C) amperometric response of CuO/CFF electrode at different potentials in 100 mM NaOH solution with a dropwise addition of 40 μM glucose; (D) the relationship between the current and applied potential.

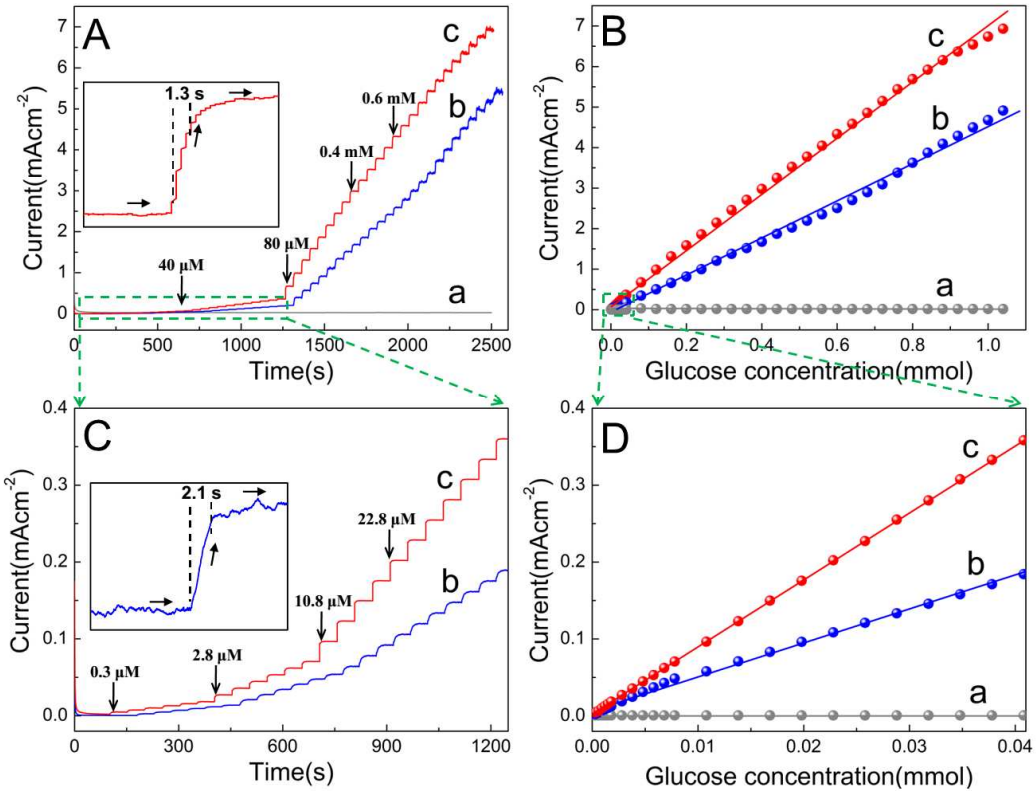

Fig. 8 Amperometric response (A) with successive addition of glucose to 100 mM NaOH solution per 50 s at 0.45 V and calibration curves (B) of current response versus glucose concentration at the bare CFF (a), CuO/G (b) and CuO/CFF (c) electrodes; the enlarged part on the response current in Fig. 8A (C) and in Fig. 8B (D) toward low glucose concentration. The response time of the CuO/CFF electrode (inset in Fig. 8A) and the CuO/G electrode (inset in Fig. 8C) with injection of 40 μM glucose.

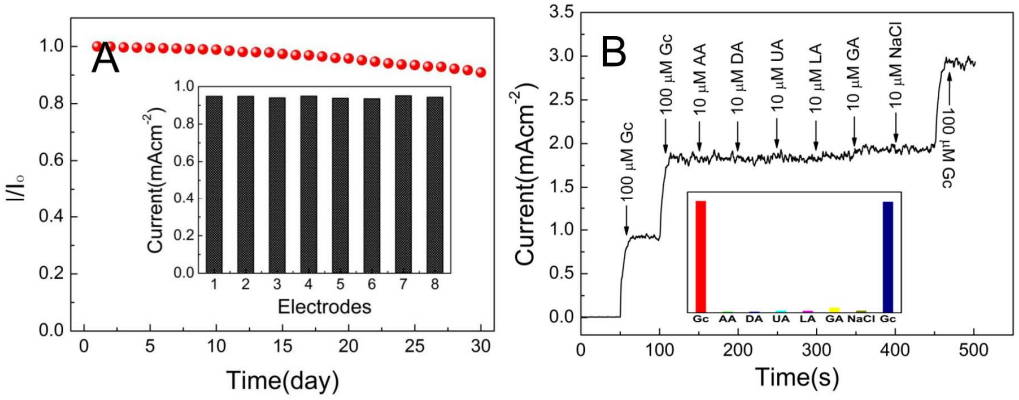

Fig. 9 (A) Long-term stability in sensitivity of CuO/CFF electrode electrode during a period of 30 days; (B) amperometric response to sequential addition of 100 μM glucose and 10 μM interfering species of AA, DA, UA, GA, LA and NaCl at applied potential of 0.45 V. Inset in Fig. 9(A) shows the comparison in sensitivity of the eight CuO/CFF electrodes fabricated identically with successive addition of 0.1 mM glucose into stirred 100 mM NaOH solution at applied potential of 0.45 V; Inset in Fig. 9(B) displays selectivity of CuO/CFF sensor for electroactive interferents.